Nuclear Materials and Energy 9 (2016) 581–586

Contents lists available at ScienceDirect

Nuclear Materials and Energy

journal homepage: www.elsevier.com/locate/nme

Effects of stacking fault energies on the interaction between an edge dislocation and an 8.0-nm-diameter Frank loop of self-interstitial atoms

S. Hayakawa[a,*], Y. Hayashi[a], T. Okita[b], M. Itakura[c], K. Suzuki[b], Y. Kuriyama[b]

[a] School of Engineering, the University of Tokyo, 7-3-1 Hongo, Bunkyo, Tokyo, Japan, 1138656
[b] Research into Artifacts, Center for Engineering, the University of Tokyo, 5-1-5, Kashiwanoha, Kashiwa, Chiba, Japan, 2778568
[c] Center for Computational Science & e- Systems, Japan Atomic Energy Agency, 178-4-148-4, Wakashiba, Kashiwa, Chiba, Japan, 2770871

ARTICLE INFO

Article history:
Available online 26 October 2016

Keywords:
Molecular dynamics
Radiation-induced degradation
Shear band
Austenitic stainless steels

ABSTRACT

Molecular dynamics simulations were conducted to investigate the effects of stacking fault energy (SFE) as a single variable parameter on the interaction between an edge dislocation and a Frank loop of self-interstitial atoms with a diameter of 8.0 nm. The physical contact between the edge dislocation and the loop causes constriction of the edge dislocation, followed by the formation of a D-Shockley partial dislocation. The latter process is associated with either the formation of a screw component and its cross-slip, or the direct core reaction between the dislocation and the loop. These processes induce either the absorption of the loop into the dislocation or the transformation of the loop into a perfect loop. The SFE influences the interaction morphologies by determining the separation distance of the two partial dislocations and consequently the rate of constriction. The dependence of the interaction morphology on the SFE varies with the habit plane of the loop. A higher SFE increases the probability of the absorption or transformation interaction; however, only loop shearing is observed at the lower limit of the SFE range of austenitic stainless steels.

1. Introduction

In austenitic stainless steels, which are used as in-core structural materials of light water reactors (LWRs), we observe two significant changes in their mechanical properties due to neutron irradiation. The first is an increase in yield stress, which is mainly caused by irradiation-induced defects impeding the glide motion of dislocations. The other is the localization of the plastic deformation in shear bands, above a certain irradiation dose. This is caused by the removal of irradiation-induced defects by dislocations that exist on or near the glide planes of the dislocation. The removal of these defects makes subsequent dislocations move more easily in these narrow regions [1]. The dominant irradiation-induced microstructures are self-interstitial atom (SIA)-type Frank loops occurring within the temperature range of LWRs [2–4]; thus, it is important to evaluate the interaction with a dislocation to investigate the micro-mechanisms responsible for the aforementioned changes.

Molecular dynamics (MD) simulations for pure face-centered-cubic (FCC) metals have shown that there are three types of interaction morphologies between an edge dislocation and an SIA-type Frank loop: loop drag, transformation, and loop shearing [5,6]. The loop drag and transformation interactions require the conversion of an SIA-type Frank loop into a perfect loop. This process is initiated by local constriction of the two partials into a dislocation, and it is completed with sweeping the stacking fault of the loop either by a single D-Shockley partial or by two Shockley partials [6]. Since the separation distance between the two partials is inversely proportional to stacking fault energy (SFE) [7], the SFE influences the probability of constriction and the resultant interaction morphology [8,9].

The SFE of austenitic stainless steels ranges from 16–25 mJ/m^2 at room temperature to 31–34 mJ/m^2 at approximately 330 °C [10], which is lower than that of other pure FCC metals such as Ni or Al. Although the SFE of Cu is as low as the upper limit of the SFE of austenitic stainless steels, the SFE of austenitic stainless steels is still lower, particularly at room temperature. Therefore, it is

* Corresponding author. Fax +81 3 5841 2904.
E-mail addresses: hayakawa@race.u-tokyo.ac.jp (S. Hayakawa), hayashi@race.u-tokyo.ac.jp (Y. Hayashi), okita@race.u-tokyo.ac.jp (T. Okita), itakura.mitsuhiro@jaea.go.jp (M. Itakura), katsu@race.u-tokyo.ac.jp (K. Suzuki), kuriyama@race.u-tokyo.ac.jp (Y. Kuriyama).

http://dx.doi.org/10.1016/j.nme.2016.10.010

necessary to evaluate the effect of the SFE on the interaction to utilize the data obtained with the Cu potential.

In this study, we conducted MD simulations by using recently developed embedded atom method (EAM)-type interatomic potentials to investigate the effect of the SFE on the interaction of an SIA-type Frank loop with a diameter of 8.0 nm with an edge dislocation. We performed a detailed analysis of the change in the interaction morphologies associated with the core reaction between the dislocation and the 8.0-nm-diameter loop.

2. Simulation methods

We used the EAM-type potentials developed by V. Borovikov et al. [11]. The SFE ranges from 14.6 mJ/m^2 to 186.5 mJ/m^2, while other material properties were kept almost identical. Four interatomic potentials with SFEs of 14.6, 24.8, 44.1, and 186.5 mJ/m^2 were used in this study. The SFEs of the three lower potentials are within the range for typical austenitic stainless steels, and the potential with the highest SFE was chosen to clarify the characteristic behavior in low-SFE metals. By using these potentials, we evaluated the effects of the SFE as a single variable parameter on the interaction between an edge dislocation and a SIA-type Frank loop.

The large-scale atomic/molecular massive parallel simulator (LAMMPS), which was developed by Sandia National Laboratories and designed for parallel computers [12], was used in this study. Fig. 1 shows a schematic diagram of the simulation cell. The *x*, *y*, and *z* axes were taken as the [1 0 −1], [1 −2 1], and [1 1 1] directions, respectively. Periodic boundary conditions were used in the *x* and *y* directions, whereas a free boundary condition was applied in the *z* direction. The cell lengths were set at 74.1, 22.3, and 22.1 nm for the *x*, *y*, and *z* directions, respectively. An edge dislocation was placed in the cell with the Burgers vector of $\vec{b} = a_0/2[10\bar{1}]$ parallel to the *x*-axis and a line parallel to the *y*-axis [13]. A hexagonal SIA-type Frank loop with the ⟨121⟩ directions on their edges was also inserted on the α-, γ-, and δ-planes (Fig. 1). The center of the loop was on the glide plane of the dislocation. The initial distance between the core of the dislocation and the loop was approximately 37 nm.

Prior to the application of shear strain, the cell was maintained at 100 K for approximately 70 ps with a pressure almost zero. The microcanonical ensemble without temperature control was chosen for the simulations. Shear stress σ_{xz} was applied to the cell by exerting forces to the upper and lower layer of the *z* planes at a constant strain rate of 4.0×10^6 s^{-1}. Time integration was performed by using the Verlet algorithm at a constant time step of 1.0×10^{-14} s. Although the time step set in this study is slightly longer than that in previous studies [5,6], we confirmed that the energy is conserved within 0.01 eV at each time step.

The common neighbor analysis (CNA) was employed for visualization [14]. In a color version, the blue regions indicate a hexagonal-closed-pack (HCP) structure, which is synonymous with a stacking fault in an FCC structure. The red regions indicate neither an FCC nor HCP structure, which describes the core of the dislocation or the loop in most cases. For the Burgers vector analysis, the dislocation extraction algorithm (DXA) was employed [15,16].

Different distributions of the initial atomic velocity sometimes resulted in different interaction morphologies [17]. Hence, we repeated the calculations at least twice for each condition by changing the random seed of the initial velocity distribution. If a significant difference in the interaction morphology was obtained (the cases of the α-plane at an SFE of 24.8 mJ/m^2 and those of the γ-plane at an SFE of 186.5 mJ/m^2), we conducted up to five repeated calculations, and all the obtained interaction morphologies and their reaction probabilities are presented in the results section.

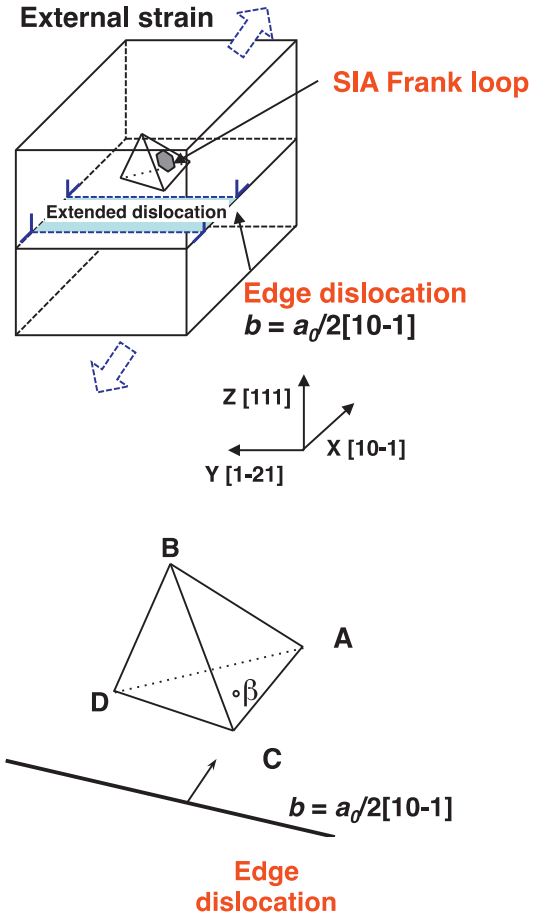

Fig. 1. Schematic diagram of the simulation cell. The Burgers vector of the dislocation follows the CA direction in the Thompson tetrahedron. The planes BCD, ABD, and ABC are denoted by the Greek letters α, γ, and δ, respectively.

Table 1
Summary of the interaction morphologies. *S*, *D*, and *T* denote the loop shearing, drag, and transformation, respectively.

SFE (mJ/m^2)	14.6	24.8	44.1	186.5
α-plane	*S*	*S* or *D*	*D*	*D*
γ-plane	*S*	*S*	*S*	*D* or *T*
δ-plane	*S*	*S*	*S*	*S*

3. Results

Table 1 summarizes the interaction morphologies for each habit plane. The probability of loop shearing increases with decreasing SFE. In the following subsections, we will show the effect of the SFE on the detailed interaction morphologies in each habit plane.

3.1. Interaction of the loop on the α-plane

Fig. 2 shows snapshots of the interaction on the α-plane at an SFE of 44.1 mJ/m^2. When the dislocation starts to move and approaches the loop because of the applied shear strain, the leading partial bends owing to the repulsive interaction (Fig. 2(a)). Then, the dislocation physically touches the loop, which locally constricts the dislocation at its top, where the screw component is formed (Fig. 2(b)). The dislocation starts to cross-slip on the plane along the loop edge, which is different from the original slip plane.